Biosensors and Bioelectronics 26 (2011) 3391–3397

Contents lists available at ScienceDirect

Biosensors and Bioelectronics

journal homepage: www.elsevier.com/locate/bios

Improved protein detection on an AC electrokinetic quartz crystal microbalance (EKQCM)

Robert Hart[a], Erten Ergezen[a], Ryszard Lec[a], Hongseok "Moses" Noh[b,*]

[a] School of Biomedical Engineering, Science & Health Systems, Drexel University, United States
[b] Department of Mechanical Engineering & Mechanics, Drexel University, 3141 Chestnut St., Rm. 2-115, Philadelphia, PA 19104, United States

ARTICLE INFO

Article history:
Received 30 September 2010
Received in revised form
14 December 2010
Accepted 27 December 2010
Available online 31 December 2010

Keywords:
AC electrokinetics
AC electroosmosis
Mixing
Quartz crystal microbalance
Protein detection

ABSTRACT

Microscale electrodes supplied with an AC field can generate rotational fluid patterns known as AC electroosmosis. In the present study, this effect was used to improve antibody binding on a biosensor surface. Antibodies, like many other large, slow moving biomolecules, tend to suffer from transport limitations during a reaction with a surface-bound receptor. Stirring such reactions with AC electroosmosis can alleviate this transport limitation by bringing fresh reagent to the surface. For the first time, the use of this phenomenon was used to improve the capture of protein on a sensor. Directly adsorbed antibodies were bound to the surface of specially modified quartz crystal microbalances, known as electrokinetic QCMs (EKQCMs) and the signal was enhanced by about 5.6 times. Modification of the QCM resulted in little reduction of quality factor (from ~5.3k to ~4.6k) and an increased sensitivity to viscosity changes (151%). Full immunoassays performed on electrodes fabricated on glass surfaces were used to ensure antibody function was not significantly degraded by the enhancement technique.

1. Introduction

Biosensors often suffer from long detection times due to the slow transport of biomolecules onto the transducer surface creating a need, especially in microfluidic systems, for a method of continuous active mixing (Beumer et al., 1996; Bange et al., 2005; Zimmermann et al., 2005). In the microfluidic regime, the low Reynolds numbers preclude turbulent mixing and few active mixing options exist. In this article, the use of AC electroosmosis (ACEO) as a method for enhancing transport of protein to a transducer surface is investigated. ACEO is an electrokinetic phenomenon characterized by stable rotational velocity patterns that exist near the surface (less than a few hundred microns) of microelectrodes (Fig. 1 (left)) (Oh et al., 2008). These rotational patterns can be used to stir the bulk solution in a microchannel which will help reduce sensor detection time. A reduction in detection time is often accompanied by a practical increase in sensitivity since a small, but rapid signal may be more easily distinguished from long term drift. Both a decrease in detection time and an increase in sensitivity can help aid translation of biosensor systems, thereby strengthening their impact on point-of-care diagnostics, environmental monitoring and counterterrorism (Owen, 1993; Wang, 2004; Ali, 2005; Bogue, 2007).

Quartz crystal microbalances (QCMs), were selected as a test sensor because they are well-studied, robust and planar, which allows for easy modification with microfabrication (O'Sullivan and Guilbault, 1999; Michalzik et al., 2005; Ricci et al., 2007). QCMs were modified by replacing the continuous circular electrode with a pair of interdigitated microelectrodes (IDEs), which can generate ACEO (Fig. 1 (right)). This new sensor–actuator type is termed 'EKQCM' (electrokinetic quartz crystal microbalance). Immunoglobulin G (IgG), a ubiquitous protein used in most immunoassays was used in a direct adsorption assay on the surface of an EKQCM using the dip-dry method to demonstrate proof of concept. By using FITC-labeled IgG fluorescent microscopy could be used to gain an understanding of the IgG spatial distribution on the sensor surface. A qualitative comparison of mixed and unmixed sensors could then be made. The results from the EKQCM experiments were also compared with predictions made by a convection–diffusion finite element simulation.

The IDEs required to generate ACEO are simple and inexpensive to fabricate and can be incorporated onto most MEMS materials (plastic, glass, silicon, etc.). Voltage and power requirements are quite low – less than 5 V_{pp} (volts peak to peak) and 10 mW respectively. Furthermore, the electrodes can be made thin (tens to hundreds of nanometers), optically transparent (for example, using indium tin oxide) and do not generate much heat (Green et al., 2001). The operational frequency for ACEO is in the kilohertz to sub kilohertz range which is often far enough away from that of many sensor types, allowing for tandem sensor-ACEO operation. The major drawback of ACEO is that it can function only in low

* Corresponding author. Tel.: +1 215 895 2273; fax: +1 215 895 1478.
E-mail address: mosesnoh@coe.drexel.edu (H.. Noh).

0956-5663/$ – see front matter © 2010 Elsevier B.V. All rights reserved.
doi:10.1016/j.bios.2010.12.038

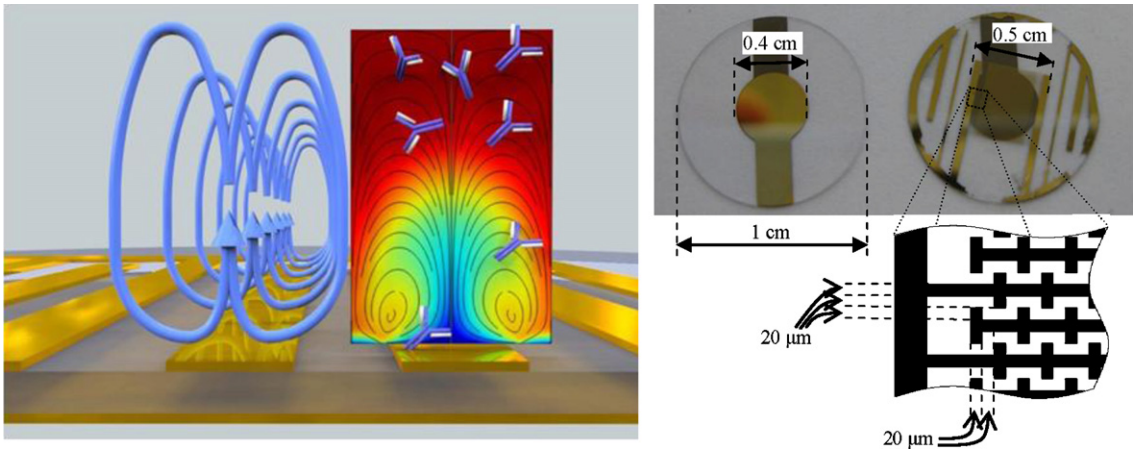

Fig. 1. Left: A conceptual diagram of ACEO motion (blue arrows) produced by parallel interdigitated electrodes and its effect on analyte concentration (color map) which is removed from the bulk solution by a reaction at the bottom surface. Right: Image of (left) an unmodified QCM and (right) a QCM that has been modified with a microelectrode pattern. The QCMs used were 1 cm in diameter and 167 μm in thickness. (For interpretation of the references to color in this figure legend, the reader is referred to the web version of this article.)

conductivity solutions. This technology will therefore be limited to applications where the analyte exists in non-buffered water or where it can be rapidly extracted from highly buffered physiological media using filtration or dialysis. This shortcoming cannot be easily overcome using ACEO although there are other electrokinetic phenomena that exist in higher conductivity media such as electrothermal effect. Though the focus of this investigation was for the detection of IgG, the results should be relevant to most proteins, nucleic acids and other biomolecules with low diffusion coefficients.

1.1. AC electroosmosis

When an IDE is submerged in an aqueous solution, an electric double layer will form upon application of a potential between the electrodes. Because the field is non-uniform, (and has a component tangential to the surface) free charges within the double layer will translate across the surface (Morgan and Green, 2002). These moving charges interact with the fluid through viscous drag and cause fluid motion. The result is a stable rotational velocity pattern depicted in Fig. 1 (left). Fluid velocities at the surface can reach up to 1 mm/s but die out with distance, causing little motion a few hundred microns away. A more thorough explanation of the mechanics of ACEO including a mathematical discussion can be found in an earlier work (Oh et al., 2008).

In addition to ACEO, there are two other common AC electrokinetic phenomena, the electrothermal effect (ETE) and dielectrophoresis (DEP). The ETE is caused by the movement of free charges that are induced by temperature gradients caused by joule heating within the fluid. The movement of these free charges within the bulk solution results in rotational velocity patterns. The ETE typically exists in high conductivity solutions and has already been investigated for use in improving heterogeneous immunoassays (Sigurdson et al., 2005; Feidman et al., 2007). DEP, unlike the other two effects, acts directly on submerged particles which move toward or away from high electric field gradients. Unfortunately, DEP cannot be easily used for molecular manipulation (though some exceptions exist (Ueda et al., 1997; Bakewell and Morgan, 2006; Hoeb et al., 2007)) and is typically reserved for handling much larger particles (cells, bacteria, viruses, etc.).

ACEO is commonly generated with IDEs that are parallel and straight. However, a variety of other designs produce ACEO with different patterns of fluid motion. In this investigation, the castellated design (Fig. 1 (right)) was used because the periodic corners can introduce more folds and bends into the fluid, enhancing the mixing capability.

1.2. The transport limited system

Transport-limited systems occur because of the small diffusion coefficients of most biomolecules, the relatively long distances these molecules need to travel and the rapid reactions that take place at the capture surface. In other words, the reactants near the surface are quickly consumed and are not adequately replenished by fresh reactants which are slow moving and far away from the surface. The result is long binding and detection times which can be improved by adequate mixing. Fig. 1 shows a conceptual representation of a mixed (with ACEO) surface reaction on an interdigitated microelectrode. An unmixed case would be represented as a one dimensional concentration gradient with a depletion layer at the surface.

A system can also be reaction rate-limited if diffusion rates are high, travel distances are small and the reaction rate is slow. To gauge whether a system is reaction rate-limited or transport-limited, a dimensionless number known as the Damköhler number (Da) can be used. This is the ratio of reaction rate to the transport rate. $Da \gg 1$ indicates a system that is highly transport-limited whereas a $Da \ll 1$ indicates a system that is highly reaction rate-limited. Even in microchannels where the diffusion distance is not great, the Da can be on the order of 100 or higher (Hu et al., 2007).

Several other groups have investigated methods of stirring reactions in the microfluidic regime using other methodologies. In general, these methods fall under three categories, electrokinetic, acoustic and magnetic. In the first category, both traditional electroosmosis (using DC voltage) (Leu and Ma, 2005; Lynn et al., 2008) and the electrothermal effect (Sigurdson et al., 2005; Feidman et al., 2007) can be used to generate rotational velocity patterns in a microchannel. Acoustic methods typically rely on acoustic streaming (Vivek et al., 2000; Liu et al., 2003; Jang et al., 2007), acoustical actuation of microbubbles, or sensor–actuators such as capacitive micromachined ultrasonic transducers (Ramanaviciene et al., 2010). Magnetic fields have also been used to actuate the fluid, either through suspended magnetically susceptible particles (Lynn et al., 2008) or via magnetohydrodynamics.

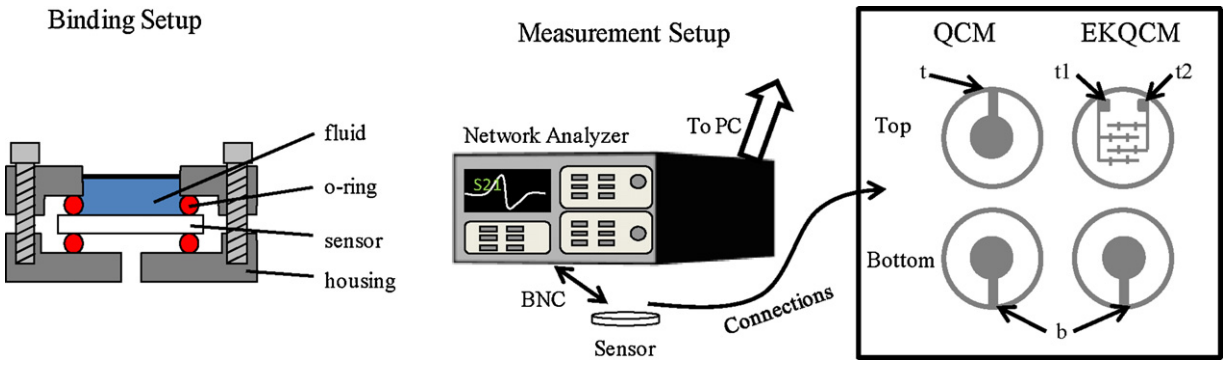

Fig. 2. A schematic of the binding setup and measurement system setup. Left: The binding setup consists of a sensor in a brass housing coated with Teflon. A fluid compartment is made water-tight with o-rings. Right: The measurement setup consists of a network analyzer connected to the sensor with BNC cables. The leads of the cables are connected to the contact pads on the sensors. For the normal QCM pads 't' and 'b' are used. For the EKQCM two cases were tested. Case 1 – 't1' and 'b' are used; case 2 – the same connections except 't1' and 't2' are shorted.

1.3. Quartz crystal microbalance

A QCM is a piezoelectric resonator that has been widely used as a biosensor and has been shown to be capable of detecting both large and small particles such as bacteria (Su and Li, 2004; Li and Xiao-Li, 2005; Ricci et al., 2007), viruses (Uttenthaler et al., 2001; Chunyan et al., 2008; Chen et al., 2009), and proteins (Kurosawa et al., 2004; Park et al., 2004; Michalzik et al., 2005). It consists of a thin disk of AT-cut quartz sandwiched between two electrodes, usually made of gold. Application of an AC current at its resonance frequency produces a standing shear wave. A change in the surface-bound mass will result in a shift in resonance frequency. In vacuum conditions or in air, the change in frequency is directly proportional to mass and can be accurately estimated using the well-known Sauerbrey equation (Sauerbrey, 1959).

2. Materials and methods

2.1. QCM modification

QCMs were modified by replacing one circular electrode with a pair of interdigitated electrodes (Fig. 1 (right)). The process started with a 10 MHz QCM (100 nm Au/10 nm Ti) (International Crystal Manufacturing). One side of the QCM was protected with Kapton tape while the electrode on the other side was removed with gold etchant (Transene Company Inc.) and 1% buffered oxide etchant (Transene Company Inc.) in deionized water to remove the Au and Ti layers respectively. This leaves one surface of the QCM completely bare and allowed for a new electrode to be patterned by the commonly used lift-off microfabrication technique. Photolithography was performed with Futurrex NR-7 negative photoresist to generate an electrode pattern on the quartz crystal. This was followed by thermal evaporation of 10 nm of Cr and 100 nm of Au. Lift-off was performed in Acetone (which removes the photoresist and the unwanted Cr and Au). This was followed by a DI water rinse, a 1 min cleaning in piranha solution (7:3 H_2SO_4:H_2O_2) and another DI water rinse. Samples were blown dry with N_2 gas.

2.2. Measurement system and calibration

Measurement of the QCMs with fundamental frequency of 10 MHz was carried out using a network analyzer (HP4395A) connected to a PC with a GPIB/USB cable. The experimental setup is shown in Fig. 2. The QCMs were placed in a custom-built brass housing with a Teflon coated fluid chamber. Thin gold wires were passed between o-ring seals and the QCM contact pads to make an electrical connection (Fig. 2 (left)). These wires were connected to the ports of the network analyzer with SMA cables. Throughout the experiments, amplitude and phase responses of the forward transmission parameter (S_{21}) were monitored. The connections to the sensor and IDE were made according to the diagram in Fig. 2 (right). Resonance frequency was obtained with in-house software programmed using LabVIEW. The software measured the S_{21} parameter using a 5 kHz span and 1 kHz bandwidth near the resonance frequency. Measurements were performed in air both before and after the antibody binding step. Air measurement of resonant frequency was made by finding the 0° phase crossing point using a least squares linear fit method.

To verify that the interdigitated electrodes did not significantly affect sensor function, a calibration was performed by applying aqueous concentrations (0%, 10%, 20% and 30%) of glycerin to one surface of modified and unmodified QCMs. QCMs were tested both before modification and then afterwards. To predict the frequency shift of the QCM to the different concentrations of glycerin, a Mason transmission line model (TLM) was used. This is a representation of the physically based one-dimensional wave and piezoelectric constitutive equations and boundary conditions (Rosenbaum, 1988). In this model, the piezoelectric crystal is represented with two acoustic ports and one electric port. Then a non-piezoelectric layer (the liquid) is represented by a 2×2 matrix, which converts material properties and acoustical parameters to electrical parameters and vice versa. Acoustic impedance can be determined by calculating the output current and voltage as a linear function of the input current and voltage and the acoustic parameters of the layers (Granstaff and Martin, 1994). This acoustic impedance is equal to the motional arm impedance of the Butterworth–Van Dyke (BVD) equivalent circuit of a QCM sensor (Fig. 3 (left)) (Bandey et al., 1999).

2.3. Antibody adsorption assays

2.3.1. Antibody detection on EKQCM

Antibody binding onto the surface of the EKQCMs was measured using the dip-dry technique, which entails comparing the resonance frequency of the sensor before and after a period of binding. Since both measurements are made in air, the Sauerbrey equation can be used to calculate the mass change based on the frequency shift. EKQCMs were first cleaned by immersing them in methanol, acetone and then isopropanol for 10 min each, followed by drying under N_2 gas. Next, the EKQCMs were placed in piranha solution (7:3 H_2SO_4:H_2O_2) for 1 min at 80 °C, followed by a 10 min immersion in deionized water. A final wash in ethanol was followed by another drying step and a bake in an 80 °C oven for 30 min.

In order to accurately control the conductivity of the antibody solution, which has a large impact on ACEO, the antibody solution

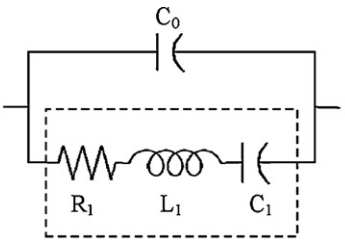

Parameter	QCM	EKQCM 1 finger	EKQCM 2 fingers
R_1 (Ω)	6.65	23.63	7.87
C_1 (fF)	27.97	27.60	27.69
L_1 (mH)	9.10	9.19	9.16
C_0 (pf)	7.13	5.84	7.16
Q	5318	4596	5278
Δf (kHz)	-	-23.90	-22.53

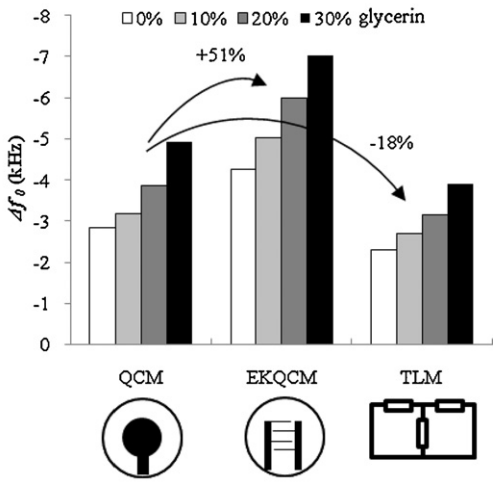

Fig. 3. Left: Electrical equivalent circuit of QCM sensor and corresponding values for the different sensors. C_o is the static capacitance of quartz, C_1, R_1 and L_1 are the intrinsic capacitance, resistance and inductance of quartz respectively. Right: Frequency response of the QCM and EKQCM to varying aqueous concentrations of glycerin. A prediction made by the transmission line model (TLM) is in the final column group.

was dialyzed in a bath of appropriately prepared DI water. Deionized water was adjusted to 2 μS/cm using potassium chloride while monitoring with a conductivity meter (Orion 105A ThermoFisher, Waltham MA). A 20 kDa-cutoff dialysis cartridge (ThermoFisher) was first hydrated for 1 min in the 2 μS/cm water. Next, 300 μl of 0.1 mg/ml fluorescein-labeled affinity-purified polyclonal goat anti-rabbit IgG (Sigma–Aldrich, St. Louis MO) in PBS (6.7 mM phosphate, 0.15 M NaCl, pH 7.4 ThermoFisher) was injected into the cartridge and allowed to incubate in a beaker of 2 μS/cm water for 2 h. The solution was replaced after 1 h since the conductivity of the water in the beaker will increase slightly due to the dialysis. IgG solution was then removed from the cartridge and diluted to 0.01 mg/ml using the same 2 μS/cm water as a diluent.

To perform the dip-dry experiment, the resonance frequency of eight EKQCMs was measured and a 50 μl droplet of antibody solution was pipetted directly onto the surface of each sensor for 15 min. ACEO mixing was applied to four of the EKQCMs by supplying the IDE with a 2 V_{pp}, 100 Hz signal. The other four interdigitated electrodes remained inactive to serve as controls. The liquid from each device was then carefully aspirated and saved. Next, the EKQCMs were washed in deionized water 3 times and dried under N_2. This was followed by another resonance frequency measurement and imaging with fluorescent microscopy (Nikon Eclipse ME600 upright microscope).

The saved solutions from each QCM were then subjected to a protein quantification assay (MicroBCA, ThermoFisher–accurate to 0.5 μg/ml). By comparing the concentration of the initial solution to the solutions after they had been applied to the QCM surfaces, the amount of adsorbed protein could be determined. A standard curve of IgG was prepared in 2 μS/cm water in a transparent 96-well corning plate. Samples from the QCMs were added to the well plate and all samples were mixed with MicroBCA reagents and incubated for 1 h at 37 °C. After 5 min of cooling, the absorbance of each well was measured using a plate reader (Tecan Infinite M200) at 562 nm. The linear fit R^2 value was 0.999.

2.3.2. Immunoassay on functionalized surface

The ability of IgG to retain its function after subjection to dialysis and high strength electric fields (up to 100 kV/m) is vitally important for future applications. This was tested with fluorescent immunoassays performed on IDEs fabricated on glass substrates. The immunoassays consist of (1) functionalizing the surface of a sensor with direct adsorption of 0.001 mg/ml nonspecific rabbit IgG (Sigma–Aldrich) in PBS for 2 h, (2) blocking with 1% BSA in PBS overnight and (3) labeling with 0.001 mg/ml fluorescently labeled secondary antibody in PBS for 2 h. A short incubation with ACEO was substituted for either the first step (case 1) or the third step (case 2) with the other steps remaining the same. In the steps using ACEO, PBS solution was replaced with 2 μS/cm water using dialysis and incubation times were reduced to 15 min. Case 1 shows whether a protein (the primary antibody) may be first subjected to ACEO and then successfully labeled. Case 2 shows whether a protein (the secondary antibody) may be successfully captured by a receptor layer in the presence of ACEO. Both cases were compared to unmixed samples that received similarly short, 15 min incubations. After all antibody binding steps, the solutions were removed and the sensors were washed carefully with DI water to remove the unbound protein. Since the functionalization is accomplished with direct adsorption, it should be noted that the antibody orientation is not controlled and that protocol simplicity has been achieved at the cost of reduced binding capacity. By using a self assembled monolayer of protein G or by a variety of other conjugation methods this binding capacity can be improved upon.

3. Results and discussion

3.1. Electrical testing and calibration

The electrical equivalent circuit for a QCM is shown in Fig. 3 (left). Using the impedance analyzer mode of the HP4395A, values for R_1, C_1, L_1, and C_0 were extracted from a standard QCM as well as for the EKQCM. The EKQCM could be operated using just one of the top electrode fingers or by shorting the top two electrodes. Both cases were measured and the equivalent circuit values are shown in Fig. 3 (left). Compared to the shorted top electrode option, the single-finger operation has greater electrical losses at resonance, which is explained by the high R_1 value. The quality factor (Q), which was determined by taking (f_0/bandwidth at −3 dB), is quite high for all cases and is only slightly negatively affected by the alteration to the top electrode. Using only one finger reduced the Q by about 14% from the original. Q was calculated by dividing the resonance frequency by the span at −3 db from resonance amplitude.

A simple prediction of the resonance frequency shift that would be caused by modification of the QCM ($\Delta f_0 = f_{0\text{-original}} - f_{0\text{-modified}}$) can be made using the Sauerbrey equation. Typically used for esti-

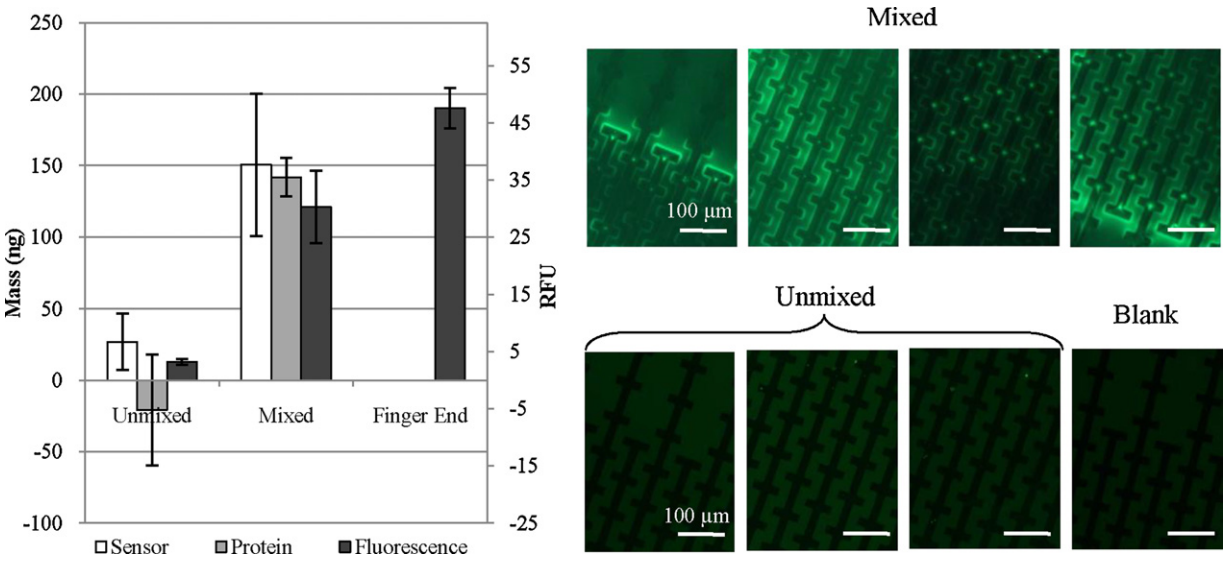

Fig. 4. Measurement of directly adsorbed fluorescein-labeled IgG bound to the EKQCM surface. The graph shows the quantity of adsorbed protein using three different measurement approaches. The three techniques are (1) EKQCM, (2) the MicroBCA protein quantification assay and (3) fluorescence microscopy. Note that the fluorescence series uses the secondary axis on the right in relative fluorescence units (RFU) and is the only method that can measure values at the finger end. The others are bulk measurement techniques. The images show mixed samples, unmixed samples and a blank, which was not subjected to any fluorescent IgG (EKQCM $n = 4$, MicroBCA assay (unmixed $n = 4$, mixed $n = 2$) and fluorescence $n = 10$)).

mating deposition of mass on the surface, the Sauerbrey equation predicts a linear relationship between resonance frequency and deposited mass. According to this equation, the sensitivity of the 10 MHz QCM is about 2.89 Hz/ng. The original electrode area was 7.85E−6 m^2 and its thickness was 100 nm of gold and 10 nm of titanium. This solid electrode was replaced with a set of castellated electrodes, the pattern of which has a spatial coverage of about 50% compared to the solid electrode (100%). The castellated electrode was made from 100 nm Au and 10 nm Cr. The difference in mass between the original and modified QCM will be about 7.5 μg, which would cause a 21.68 kHz frequency shift. (This calculation only considers the acoustically active region that overlaps with the bottom electrode and ignores the parts of the top electrode that do not overlap). The experimental resonance frequency shift that occurred during the fabrication process is shown in the last row and differs from the predicted frequency shift by about 10% for the single-finger operation and by 4% for the dual-finger operation.

QCMs are also sensitive to changes in the viscosity and density of a fluid in contact with the transducer surface. In order to ensure that the EKQCM can still function similarly to an unmodified QCM, different aqueous concentrations of glycerin were applied to the sensors and the resonance frequency shift was measured ($\Delta f_0 = f_{0\text{-liquid}} - f_{0\text{-air}}$) and compared. The transmission line model, detailed in Section 2.2 was also employed and the simulation results are shown alongside the empirical data in Fig. 3 (right). The three data sets show a similar relationship to the different concentrations, though with varying sensitivity. Compared to the QCM, the EKQCM was approximately 51.4% more sensitive while the transmission line model predicted a sensitivity of approximately 18.2% less. The TLM prediction does not account for certain experimental parameters such as QCM surface roughness, damping from the sensor housing, etc. which can explain the difference (Bandey et al., 1999). If the values for each technique were normalized by compensating for sensitivity differences, the greatest error between techniques for a given concentration would be less than 3.2%.

3.2. Measurement of antibody binding on the EKQCM

A comparison of the mixed and unmixed EKQCMs for a 15 min incubation in 0.01 mg/ml fluorescein-labeled IgG is shown in Fig. 4 (left). The EKQCM response was converted from frequency to mass using the Sauerbrey equation. The adsorbed mass provided by the MicroBCA protein quantification assay was calculated by comparing the concentrations of the solution before and after the 15 min incubation. The concentration 'lost' during this process was considered to be adsorbed onto the surface and was converted to mass and plotted. The negative value for the unmixed sample is due to measurement error and can be considered close to zero. According to the EKQCM data, in the 15 min incubation, the amount of mass adsorbed was increased by a factor of about 5.6 by utilizing ACEO mixing.

In addition to these quantitative methods, which closely agree, fluorescent photomicrographs are provided and show good qualitative agreement as well. Fluorescent intensity was also measured from 10 locations for each condition and the average value is plotted in Fig. 4. Background fluorescence was subtracted using measurements from the blank sample, which was not reacted with protein. The fluorescence micrographs indicate a fluorescent enhancement of 9.5 in the middle of the device and 14.9 at the electrode fingers. Interestingly, the antibody is preferentially adsorbed near the edges of the activated electrodes and also toward the ends of each finger–a pattern that usually indicates DEP. Furthermore, there are spots of high antibody intensity at the center of the castellated 'cross' regions, which is highly indicative of ACEO particle collection. This might indicate the possibility of agglomerated IgG, the increased size of which would make them more susceptible to DEP. Fluorescence intensity is also much higher at the ends of each finger – an effect likely caused by the 'access' the finger has to IgG past the end of the finger. Images of polystyrene microspheres under the influence of AC electrokinetic forces that show similar collection patterns were discussed in a previous work (Oh et al., 2008).

3.3. Enhanced binding of primary and secondary antibody using AC electrokinetics

In order to perform selective detection of an antigen, a biosensor must first be functionalized with a receptor layer. Results so far have only indicated the ability of ACEO to enhance nonspecific binding and do not indicate whether the antibodies have retained function after subjection to high electric fields and dialysis. To test

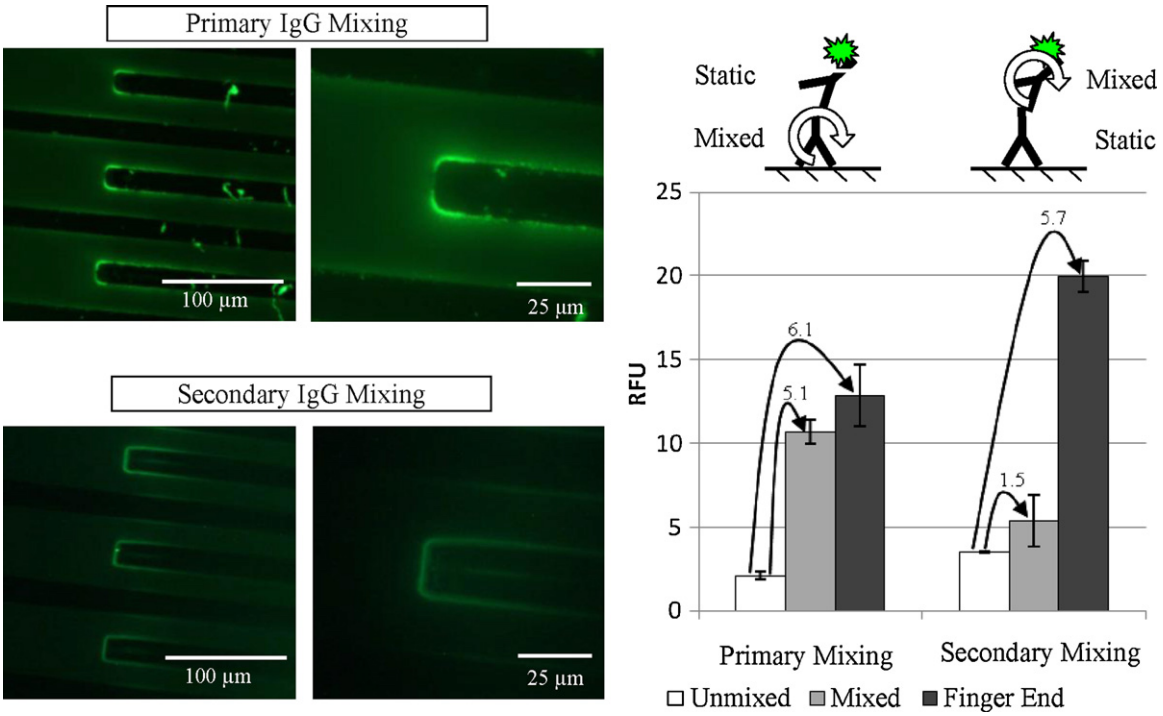

Fig. 5. Fluorescent immunoassays performed on IDEs with AC electrokinetic mixing. "Primary Mixing" refers to the use of AC electrokinetic mixing to the directly adsorbed primary antibody followed by unmixed binding of the secondary antibody. "Secondary Mixing" refers to the case for unmixed binding of the primary antibody and the use of AC electrokinetic mixing for the secondary antibody. Left: Images from immunoassays for both cases. Right: Fluorescent intensity measurements. The white bars labeled "Unmixed" were negative controls where both binding events were unmixed. Background fluorescence was removed by measuring a blank sample. Labeled arrows show an enhancement factor from the unmixed sample (unmixed $n = 4$, mixed $n = 4$, and finger end $n = 3$).

this, the assays described in Section 2.3.2 were carried out and the results are shown in Fig. 5. Like the direct adsorption assay, antibody attachment around the edges of the electrode is much more pronounced and collection at the finger ends is also much greater than in the center of the device. In both cases, fluorescent signal near the finger ends is enhanced by about 6 times. However, in the center of the device, mixing during the primary IgG binding step was much more effective than during the secondary step.

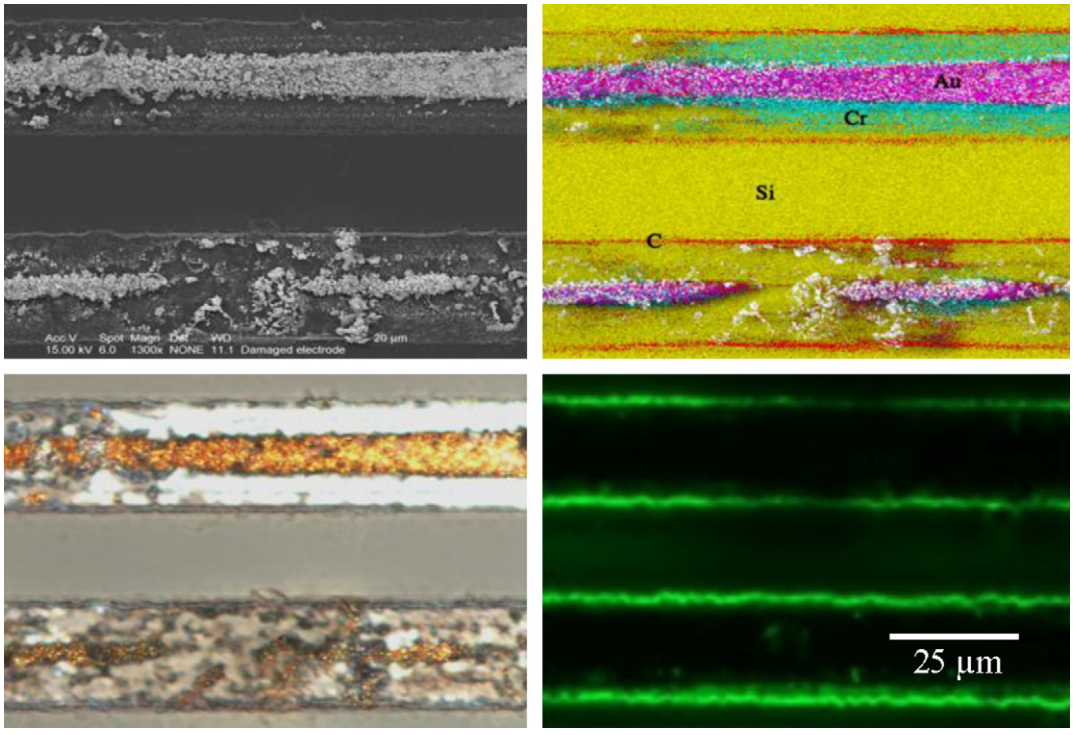

Fig. 6. The same location on the device was analyzed with four different techniques: scanning electron microscopy (top left), energy-dispersive X-ray analysis (top right), light microscopy (bottom left) and fluorescent microscopy (bottom right).

3.4. Electrode damage at high voltages

Throughout the experiments, a voltage of 2 V_{pp} was applied to the electrodes to induce electroosmotic mixing. The maximum field strength in this case is about 100 kV/m. Increasing voltage has the clear effect of increasing antibody collection on the electrodes. However, voltage cannot be raised indefinitely due to electrolysis of water and damage to the electrode itself. Others have reported similar findings without investigation (Bakewell and Morgan, 2006; Park and Beskok, 2008). It was noted that 5 V_{pp} (field strength of about 250 kV/m) or greater caused visible electrode damage. It was therefore decided that voltages no higher than 2 V_{pp} would be used. The mechanism of this damage is currently unknown but, like electrolysis of water, the electrode damage is dependent on voltage and frequency and it seems likely that this is due to some electrochemical reaction. Lower frequencies and higher voltages are more likely to damage the electrode. Interestingly, this damage also is related to the antibody concentration. Higher concentrations of antibodies in solution are more likely to damage the electrodes. To study this phenomenon, a straight parallel IDE (20 μm electrode width and 20 μm gap width) was severely damaged by applying a 10 V_{pp} 100 Hz signal for 30 min using an antibody concentration of 0.1 mg/ml with a solution conductivity of 1 μS/cm. Images of the damaged device using four different modalities are shown in Fig. 6. In some locations, both the gold and the chromium layers are removed, and in others, only the gold. Antibodies are accumulated on the electrode edges even when the electrode is no longer there.

4. Conclusion

For the first time, ACEO has been used to improve detection of protein on a biosensor. For proof of concept this was shown using a conventional batch mode approach and may be later incorporated into a microfluidic system by miniaturizing the sensing region and enclosing it within a microfluidic channel (for example, using PDMS). Using this phenomenon as a means of stirring diffusion-limited adsorption of protein onto a transducer surface resulted in an increase of bound protein by a factor of 5.6. In order to accomplish this, a novel electrokinetically enhanced transducer, an electrokinetic QCM (EKQCM), was designed and fabricated. The increase in the amount of adsorbed protein was corroborated by a protein assay, as well as with fluorescent microscopy, the former agreeing with the estimated mass deposited on the EKQCM and the latter showing a bulk enhancement of 9.5 times. Near the electrode finger ends, the fluorescent intensity was greatest with an enhancement of about 14 times. Immunoassays on interdigitated electrodes were used to show that this technique did not significantly decrease protein function. ACEO was used either during the direct adsorption of primary antibody to the transducer surface (enhancement of 5.1 times in the device center and 6.1 times at the finger ends) or during the binding of secondary antibody to the primary (enhancement of 1.5 times in the device center and 5.7 times at the finger ends). ACEO mixing velocity increases with voltage which benefits performance. However, this can eventually damage the device, as evidenced by brown discoloration and removal of areas of the gold and chromium electrodes. It was considered safe to use a 100 Hz, 2 V_{pp} signal which creates a maximum 100 kV/m electric field. An applied voltage of 5 V_{pp} or higher resulted in damage and device failure.

Acknowledgements

The authors would like to acknowledge the assistance rendered by Himanshu Mehta and Nishit Mehta for their help constructing the housing into which the sensors were placed and devising the means of creating electrical connections. We would also like to thank the staff of the Drexel Materials Characterization Facility, and in particular, Dee Breger, who helped set up the SEM EDAX image exposure.

References

Ali, Z., 2005. Measurement and Control 38 (3), 87–91.
Bakewell, D.J., Morgan, H., 2006. IEEE Transactions on NanoBioscience 5 (1), 1–8.
Bandey, H.L., Martin, S.J., et al., 1999. Analytical Chemistry 71 (11), 2205–2214.
Bange, A., Halsall, H.B., et al., 2005. Biosensors and Bioelectronics 20 (12), 2488–2503.
Beumer, T., Haarbosch, P., et al., 1996. Analytical Chemistry 68 (8), 1375–1380.
Bogue, R., 2007. Sensor Review 27 (1), 7.
Chen, S.-H., Chuang, Y.-C., et al., 2009. Nanotechnology 20 (21).
Chunyan, Y., Tangyou, Z., et al., 2008. Biosensors and Bioelectronics 23, 879–885 (Copyright 2008, The Institution of Engineering and Technology).
Feidman, H.C., Sigurdson, M., et al., 2007. Lab on a Chip 7 (11), 1553–1559.
Granstaff, V.E., Martin, S.J., 1994. Journal of Applied Physics 75 (3), 1319–1329.
Green, N.G., Rarnos, A., et al., 2001. Journal of Electrostatics 53 (2), 71–87.
Hoeb, M., Radler, J.O., et al., 2007. Biophysical Journal 93 (3), 1032–1038.
Hu, G., Gao, Y., et al., 2007. Biosensors and Bioelectronics 22 (7), 1403–1409.
Jang, L.-S., Chao, S.-H., Holl, M.R., Meldrum, D.R., 2007. Sensors and Actuators, A: Physical 138, 179–186.
Kurosawa, S., Nakamura, M., et al., 2004. Biosensors and Bioelectronics 20 (6), 1134–1139.
Leu, T.S., Ma, F.C., 2005. Journal of Mechanics 21, 137–144.
Li, Y., Xiao-Li, S., 2005. Biosensors and Bioelectronics 21 (6), 840–848.
Liu, R.H., Lenigk, R., Druyor-Sanchez, R.L., Yang, J., Grodzinski, P., 2003. Analytical Chemistry 75, 1911–1917.
Lynn, N.S., Henry, C.S., Dandy, D.S., 2008. Microfluidics and Nanofluidics 5, 493–505.
Michalzik, M., Wilke, R., et al., 2005. Sensors and Actuators B: Chemical 111–112, 410–415.
Morgan, H., Green, N.G., 2002. AC Electrokinetics: Colloids and Nanoparticles. SRP Ltd, England.
Oh, J., Hart, R., Capurro, J., Noh, H.(M.), 2008. Lab on a Chip 9, 62–78.
O'Sullivan, C.K., Guilbault, G.G., 1999. Biosensors and Bioelectronics 14 (8–9), 663–670.
Owen, V.M., 1993. Sensor Review 13 (4), 3.
Park, I.-S., Kim, D.-K., et al., 2004. Biosensors and Bioelectronics 19 (7), 667–674.
Park, S., Beskok, A., 2008. Analytical Chemistry 80 (8), 2832–2841.
Ramanaviciene, A., Virzonis, D., Vanagas, G., Ramanavicius, A., 2010. Analyst 135 (7), 1531–1534.
Ricci, F., Volpe, G., et al., 2007. Analytica Chimica Acta 605 (2), 111–129.
Rosenbaum, J., 1988. Bulk Acoustic Wave Theory and Devices. Artech House, Boston.
Sauerbrey, G., 1959. Zeitschrift fur Physik 155 (2), 206–222.
Sigurdson, M., Wang, D., Meinhart, C.D., 2005. Lab Chip 5, 1366–1373.
Su, X.L., Li, Y., 2004. Biosensors and Bioelectronics 19 (6), 563–574.
Ueda, M., Yoshikawa, K., et al., 1997. Polymer Journal 29 (12), 1040–1043.
Uttenthaler, E., Schraml, M., et al., 2001. Biosensors and Bioelectronics 16 (9–12), 735–743.
Vivek, V., Zeng, Y., Kim, E.S., 2000. Proceedings of the IEEE Micro Electro Mechanical Systems (MEMS), 668–673.
Wang, J., 2004. Analytica Chimica Acta 507 (1), 3–10.
Zimmermann, M., Delamarche, E., et al., 2005. Biomedical Microdevices 7 (2), 99–110.